JOURNAL OF AIRCRAFT
Vol. 42, No. 5, September–October 2005

Dynamic Response of Aeroservoelastic Systems to Gust Excitation

M. Karpel* and B. Moulin†
Technion—Israel Institute of Technology, 32000 Haifa, Israel
and
P. C. Chen‡
Zona Technology, Scottsdale, Arizona 85251-3540

Frequency-domain and time-domain approaches to dynamic response analysis of aeroservoelastic systems to atmospheric gust excitations are presented. The discrete and continuous gust inputs are defined in either time-domain or stochastic terms. The various options are formulated in a way that accommodates linear control systems of the most general form. The frequency-domain approach is based on the interpolation of generalized aerodynamic force coefficient matrices and the application of Fourier transforms for time-domain solutions. The time-domain approach uses state-space formulation that requires the frequency-dependent aerodynamic coefficients to be approximated by rational functions of the Laplace variable. Once constructed, the state-space equations of motion are more suitable for time simulations and for the interaction with control design algorithms. However, there is some accuracy loss because of the rational approximation. The spiral nature in the complex plane of the gust-related aerodynamic terms is discussed, and means are provided for dealing with the associated numerical difficulties. A hybrid formulation that does not require the rational approximation of the gust coefficients is also presented for optional use in discrete gust response analysis. The various methods were utilized in the ZAERO software and applied to a generic transport aircraft model.

Introduction

THE design of modern flight vehicle requires the evaluation of dynamic loads in response to discrete and random gust excitations.[1] Aviation regulations define design discrete gust profiles in a deterministic manner and continuous gust profiles in a stochastic manner. Common gust response procedures, such as those of MSC/NASTRAN,[2] are based on second-order frequency-domain formulation. Modal frequency response functions are used in these procedures to calculate discrete transient gust response, via Fourier and inverse-Fourier transforms, and continuous gust response in rms terms via numerical integration of response power-spectral-density (PSD) functions.

The main advantage of the frequency-domain approach is that it is based on oscillatory generalized aerodynamic-force-coefficient (AFC) matrices that can be generated by common, well-established, commercially available procedures such as the doublet-lattice method[3] implemented in MSC/NASTRAN[2] and the constant-pressure panel method[4] implemented in ZAERO.[5] A major disadvantage of the existing frequency-domain procedures is that they are not conveniently adaptable to the consideration of control system effects on structural design gust loads and the inclusion aeroelastic gust-response considerations in the control-system design.

A common approach to aeroservoelastic (ASE) analysis is based on the conversion of the second-order aeroelastic equation of motion into first-order, state-space constant-coefficient time-domain equations of motion, which requires the approximation of the AFC matrices by rational functions in the Laplace domain. Rational approximation techniques such as the term-by-term Roger's approximation[6] and the more complicated minimum-state method[7] are well established and commercially available. However, their application might involve some problems such as degraded accuracy, excessive number of augmenting states or the need for careful parameterization, namely, loss of process robustness. Furthermore, specific difficulties might occur in the approximation of the generalized gust forces, as detailed later in this paper.

Two different formulation approaches are developed, evaluated, and compared in this paper. The first is first-order frequency-domain approach, which accommodates control systems in their most general state-space form, but with the AFC matrices still in their transcendental frequency-domain form. This option is intended for being used in industrial gust loads analysis process in which typically thousands of cases are evaluated in an automated manner, where robustness and compatibility with open-loop frequency-domain loads are of critical importance. The second approach is based on state-space time-domain formulation based on rational approximations. This option is intended for cases where time-domain simulations, possibly with nonlinear effects, are required, for representing the aeroelastic system in a control design process, and for application in design optimization processes, which are based on standard state-space formulation.

The following formulation starts with Laplace- and frequency-domain equations of motion, followed by time-domain state-space equations. Response to deterministic discrete gusts is described next, outlining various analytical options for performing the computations with their relative advantages and deficiencies. The two main formulation options are then applied to continuous-gust loads analysis. A numerical example with a simplified transport aircraft model demonstrates the various loads options and a control design process aimed at evaluating the gust loads.

Second-Order Open-Loop Equations of Motion

The Laplace transform of the open-loop aeroelastic equation of motion in generalized coordinates, excited by control surface motion and atmospheric gusts, is

$$\begin{aligned}\Big([M_{hh}]s^2 + [B_{hh}]s + [K_{hh}] + q_\infty[Q_{hh}(s)]\Big)\{\xi(s)\} \\ = -\Big([M_{hc}]s^2 + q_\infty[Q_{hc}(s)]\Big)\{\delta_c(s)\} \\ - (q_\infty/V)[Q_{hG}(s)]\{w_G(s)\}\end{aligned} \tag{1}$$

where s is the Laplace variable; q_∞ is the dynamic pressure; V is the air velocity, the left-hand-side matrix coefficient matrices are the

Received 25 November 2003; revision received 17 September 2004; accepted for publication 20 September 2004.

*Professor, Sanford Kaplan Chair in Aerospace Engineering. Associate Fellow AIAA.
†Senior Researcher. Member AIAA.
‡Vice President. Member AIAA.

generalized mass, damping, stiffness and aerodynamic AFC matrices associated with modal displacements $\{\xi(s)\}$; and the right-hand-side matrices are the mass and AFC generalized forcing matrices caused by control surface commanded deflections $\{\delta_c(s)\}$ and gust velocity vector $\{w_G(s)\}$. The AFC matrices $[Q_{\rm hh}(s)]$, $[Q_{\rm hc}(s)]$, and $[Q_{\rm hG}(s)]$ can be calculated by unsteady aerodynamic codes at various tabulated reduced-frequency k values along the imaginary axis of the nondimensional Laplace variable

$$p \equiv sL/V = g + ik \tag{2}$$

where L is the reference length. In principle, an aircraft linear control system, including the sensor and actuator dynamics, could be expressed as a matrix of transfer functions relating the control surface commanded deflections to the generalized displacements

$$\{\delta_c(s)\} = [T_{\rm ch}(s)]\{\xi(s)\} \tag{3}$$

The ASE loop could then be closed by the substitution of Eq. (3) in Eq. (1), which yields

$$\begin{aligned}&\left([M_{\rm hh}]s^2 + [B_{\rm hh}]s + [K_{\rm hh}] + q_\infty[\bar{Q}_{\rm hh}(s)]\right)\{\xi(s)\}\\ &\quad = -(q_\infty/V)[Q_{\rm hG}(s)]\{w_G(s)\}\end{aligned} \tag{4}$$

where

$$[\bar{Q}_{\rm hh}(s)] = [Q_{\rm hh}(s)] + \left([M_{\rm hc}]s^2 + q_\infty[Q_{\rm hc}(s)]\right)[T_{\rm ch}(s)] \tag{5}$$

Frequency-domain numerical schemes, originally developed for aeroelastic systems with no control augmentation, could be employed for ASE gust response analysis by simply using $[\bar{Q}_{\rm hh}(ik)]$ of Eq. (5) (with s replaced by ikV/L) instead of $[Q_{\rm hh}(ik)]$ of Eq. (1). The problem is that $[\bar{Q}_{\rm hh}(ik)]$ might cause numerical difficulties because of the control-system roots. Also, the solution of Eq. (4) does not provide any information on the response of the control elements. An alternative frequency-domain approach, which takes advantage of the state-space ASE formulation and is also compatible with the frequency-domain solutions of ZAERO,[5] is presented next.

First-Order Equations with Transcendental Aerodynamics

The time-domain part of the ASE module in the ZAERO is based on modeling the ASE problem in a constant-coefficient state-space form based on rational approximation of the AFC matrices. The control part of the modeling process transforms control components of the most general architecture into a single state-space equation that is augmented to the aeroelastic system. To facilitate a frequency-domain solution that both retains the full representation of the control equations in a first-order form and avoids the need for rational aerodynamic approximation, the state-space ASE equations are expressed in this section in the Laplace domain, with the aerodynamic coefficient matrices kept in their transcendental form. These equations can be used for frequency-domain stability and response analyses where the aerodynamic coefficients are interpolated from the database of tabulated AFC matrices.

The second-order open-loop aeroelastic equation of motion (1) can be expressed as

$$s\{x_{\rm ae}\} = [A_{\rm ae}]\{x_{\rm ae}\} + [B_{\rm ae}]\{u_{\rm ae}\} + [B_{\rm aw}]\{w_G\} \tag{6}$$

where

$$\{x_{\rm ae}\} = \begin{Bmatrix}\xi\\ s\xi\end{Bmatrix} \qquad \{u_{\rm ae}\} = \begin{Bmatrix}\delta_c\\ s\delta_c\\ s^2\delta_c\end{Bmatrix}$$

$$[A_{\rm ae}] = \begin{bmatrix}0 & I\\ -[M_{\rm hh}]^{-1}[K_{\rm hh} + q_\infty Q_{\rm hh}(s)] & -[M_{\rm hh}]^{-1}[B_{\rm hh}]\end{bmatrix}$$

$$[B_{\rm ae}] = \begin{bmatrix}0 & 0 & 0\\ -q_\infty[M_{\rm hh}]^{-1}[Q_{\rm hc}(s)] & 0 & -[M_{\rm hh}]^{-1}[M_{\rm hc}]\end{bmatrix}$$

$$[B_{\rm aw}] = \begin{bmatrix}0\\ -\dfrac{q_\infty}{V}[M_{\rm hh}]^{-1}[Q_{\rm hG}(s)]\end{bmatrix}$$

The augmentation of the actuator states[5,7] yields the open-loop plant equations excited by the actuator inputs $\{\delta_c\}$. With state-space representation of the control system, the uncoupled plant and control equations can be expressed as

$$\begin{aligned}s\begin{Bmatrix}X_p\\ X_c\end{Bmatrix} &= \begin{bmatrix}A_p(s) & 0\\ 0 & A_c\end{bmatrix}\begin{Bmatrix}X_p\\ X_c\end{Bmatrix}\\ &\quad + \begin{bmatrix}B_p & 0\\ 0 & B_c\end{bmatrix}\begin{Bmatrix}u_p\\ u_c\end{Bmatrix} + \begin{bmatrix}B_{\rm pw}(s)\\ 0\end{bmatrix}\{w_G\}\\ \begin{Bmatrix}y_p\\ y_c\end{Bmatrix} &= \begin{bmatrix}C_p(s) & 0\\ 0 & C_c\end{bmatrix}\begin{Bmatrix}X_p\\ X_c\end{Bmatrix}\\ &\quad + \begin{bmatrix}0 & 0\\ 0 & D_c\end{bmatrix}\begin{Bmatrix}u_p\\ u_c\end{Bmatrix} + \begin{bmatrix}C_{\rm Gp}(s)\\ 0\end{bmatrix}\{w_G\}\end{aligned} \tag{7}$$

where the plant state vector is $\{X_p\}^T = \lfloor \xi^T \;\; s\xi^T \;\; \delta^T \;\; s\delta^T \;\; s^2\delta^T \rfloor$, which includes the control actuator states; $\{X_c\}$ is the vector of control states; $[B_{\rm pw}]$ is $[B_{\rm aw}]$ of Eq. (6), supplemented with zero rows. The plant system matrix $[A_p(s)]$ can be expressed as

$$[A_p(s)] = [A_{\rm na}] - q_\infty[A_1][Q_{\rm hh}(s) \quad 0 \quad Q_{\rm hc}(s) \quad 0 \quad 0] \tag{8}$$

where $[A_{\rm na}]$ is the system matrix without the aerodynamic terms, which is independent of s, and $[A_1]^T = [0 \;\; M_{\rm hh}^{-1} \;\; 0 \;\; 0 \;\; 0]$. The plant output matrices in Eq. (7) are

$$[C_p(s)] = [C_{\rm na}] - q_\infty[\phi_{\rm acc}][M_{\rm hh}]^{-1}[Q_{\rm hh}(s) \quad 0 \quad Q_{\rm hc}(s) \quad 0 \quad 0]$$

$$[C_{\rm Gp}(s)] = -q_\infty[\phi_{\rm acc}][M_{\rm hh}]^{-1}[Q_{\rm hG}(s)] \tag{9}$$

where $[C_{\rm na}]$ is the output matrix without the aerodynamic terms and $[\phi_{\rm acc}]$ is a zero matrix except for modal displacement rows associated with acceleration outputs. The constant matrices $[A_{\rm na}]$ and $[C_{\rm na}]$ can be generated by the regular modeling process[5,7] with the aerodynamic terms ignored. We assume at this point that the output vector in Eq. (7) is based on sensor measurements and control outputs only. Plant outputs for calculating other gust response parameters will be added later.

The ASE loop is closed by the application of the gain matrix

$$\begin{Bmatrix}u_p\\ u_c\end{Bmatrix} = \begin{bmatrix}G_{\rm pp} & G_{\rm pc}\\ G_{\rm cp} & G_{\rm cc}\end{bmatrix}\begin{Bmatrix}y_p\\ y_c\end{Bmatrix} \tag{10}$$

The substitution of Eq. (10) in Eq. (7), using Eqs. (8) and (9), yields the closed-loop vehicle equation

$$s\{X_v\} = [\bar{A}_v(s)]\{X_v\} + [\bar{B}_{\rm vw}(s)]\{w_G\} \tag{11}$$

where

$$\{X_v\}^T = \begin{bmatrix}X_p^T & X_c^T\end{bmatrix}$$

and

$$[\bar{A}_v(s)] = [\bar{A}_{\rm na}] - q_\infty[A_2][Q_{\rm hh}(s) \quad 0 \quad Q_{\rm hc}(s) \quad 0 \quad 0 \quad 0]$$

$$[\bar{B}_{\rm vw}(s)] = -(q_\infty/V)[A_2][Q_{\rm hG}(s)] \tag{12}$$

where $[\bar{A}_{\rm na}]$ is the closed-loop system matrix with the aerodynamic terms ignored, and

$$[A_2] = \begin{bmatrix}A_1\\ 0\end{bmatrix} + \begin{bmatrix}B_pG_{\rm pp} + B_pG_{\rm pc}(I - D_cG_{\rm cc})^{-1}D_cG_{\rm cp}\\ B_cG_{\rm cp} + B_cG_{\rm cc}(I - D_cG_{\rm cc})^{-1}D_cG_{\rm cp}\end{bmatrix}\left[\phi_{\rm acc}M_{\rm hh}^{-1}\right] \tag{13}$$

Frequency-domain modal response analysis can be performed by replacing s in Eq. (11) by $i\omega$ and interpolating for the aeromatrices from the tabulated $[Q_{\rm hh}(ik)]$, $[Q_{\rm hc}(ik)]$, and $[Q_{\rm hG}(ik)]$ matrices.

State-Space Time-Domain Equations of Motion

The time-domain ASE model for gust response analysis is based on the models of Refs. 7 and 8. The formulation here assumes spanwise uniform gust velocity. However, spanwise corrections can be made in ZAERO to reflect nonuniform gust velocity distributions.

The tabulated aeromatrices are first used for approximating the AFC matrix as a rational function of k in the entire frequency domain. An expansion to the entire Laplace domain is then performed by replacing ik in the rational expression by the nondimensional Laplace variable p of Eq. (2). The resulting Laplace-domain approximation of $[Q_h]=[Q_{\rm hh}\ \ Q_{\rm hc}\ \ Q_{\rm hG}]$ is

$$[\tilde{Q}_h(s)] = [A_0] + (L/V)[A_1]s + (L^2/V^2)[A_2]s^2 + [D]\big([I]s - (V/L)[R]\big)^{-1}[E]s \tag{14}$$

where the $[A_i]$ and $[E]$ matrices are column partitioned as

$$[A_i] = \begin{bmatrix} A_{{\rm hh}_i} & A_{{\rm hc}_i} & A_{{\rm hG}_i} \end{bmatrix}, \qquad (i = 0, 1, 2)$$

$$[E] = [E_h \quad E_c \quad E_G] \tag{15}$$

To avoid coefficients associated with the second time derivative of the gust velocity, approximation constraints[5] are applied to the gust columns to yield $[A_{{\rm hG}_2}]=0$.

An augmenting aerodynamic state vector is defined by its Laplace transform as

$$\{x_a(s)\} = ([I]s - (V/L)[R])^{-1}([E_h]\{\xi(s)\} + [E_c]\{\delta_c(s)\} + (1/V)[E_G]\{w_G(s)\})s \tag{16}$$

The resulting state-space time-domain version of the open-loop Eq. (6) is

$$\{\dot{x}_{\rm ae}\} = [A_{\rm ae}]\{x_{\rm ae}\} + [B_{\rm ae}]\{u_{\rm ae}\} + [B_{\rm aw}]\{\tilde{w}_G\} \tag{17}$$

where $\{x_{\rm ae}\}$, $\{u_{\rm ae}\}$, $[A_{\rm ae}]$, and $[B_{\rm ae}]$ are defined in Refs. 5 and

$$\{\tilde{w}_G\} = \begin{Bmatrix} w_G \\ \dot{w}_G \end{Bmatrix}$$

$$[B_{\rm aw}] = \begin{bmatrix} 0 & 0 \\ -\dfrac{q_\infty}{V}[\bar{M}]^{-1}\big[A_{{\rm hG}_0}\big] & -\dfrac{q_\infty L}{V^2}[\bar{M}]^{-1}\big[A_{{\rm hG}_1}\big] \\ 0 & \dfrac{1}{V}[E_G] \end{bmatrix} \tag{18}$$

where

$$[\bar{M}] = [M_{\rm hh}] + \big(q_\infty L^2/V^2\big)\big[A_{{\rm hh}_2}\big]$$

The sensor-reading expression in Ref. 5 is expanded to include a gust noise term,

$$\{y_{\rm ae}\} = [C_{\rm ae}]\{x_{\rm ae}\} + [D_{\rm ae}]\{u_{\rm ae}\} + [C_{\rm Ga}]\{\tilde{w}_G\} \tag{19}$$

where the only nonzero rows in $[C_{\rm Ga}]$ are those associated with acceleration signals, as just shown for $[C_{\rm Gp}]$ in Eq. (9).

The plant equations, which include the actuators, become

$$\{\dot{x}_p\} = [A_p]\{x_p\} + [B_p]\{u_p\} + [B_{\rm pw}]\{\tilde{w}_G\}$$

$$\{y_p\} = [C_p]\{x_p\} + [C_{\rm Ga}]\{\tilde{w}_G\} \tag{20}$$

where $[B_{\rm pw}]^T = [B_{\rm aw}{}^T \ \ 0]$. The vehicle equations of motion with the control system augmented become

$$\{\dot{x}_v\} = [A_v]\{x_v\} + [B_v]\{u_v\} + [B_{\rm vw}]\{\tilde{w}_G\}$$

$$\{y_v\} = [C_v]\{x_v\} + [D_v]\{u_v\} + [C_{\rm Gv}]\{\tilde{w}_G\} \tag{21}$$

The equation of motion of the closed-loop aeroservoelastic system, similarly to Eq. (11), is obtained by the substitution of the gains of Eq. (10), which yields

$$\{\dot{x}_v\} = [\bar{A}_v]\{x_v\} + [\bar{B}_{\rm vw}]\{\tilde{w}_G\} \tag{22}$$

where $[\bar{A}_v]$ is the closed-loop system matrix defined in Ref. 5 and

$$[\bar{B}_{\rm vw}] = [B_{\rm vw}] + [B_v][G_v][I - D_v G_v]^{-1}[C_{\rm Gv}]$$

where $[G_v]$ is the entire gain matrix of Eq. (10). Output parameters that are not used by the control system but are of interest for dynamic response analysis can be defined as a separate vector $\{y_R\}$ and expressed in terms of the plant states, similarly to the sensor readings of Eq. (20).

Generation of a Gust Column

The formulation for generating a gust column of the gust aerodynamic matrix $[Q_{\rm hG}(ik)]$ is similar to that of Ref. 2. It is given here as a background for the discussion on its special features and their treatment in subsequent applications.

Figure 1 depicts a prescribed discrete gust profile $w_G(t)$ moving towards the flight vehicle at speed V. The reference point at which the gust profile is defined is located at $x=x_0$ along the vehicle longitudinal (x) axis. The induced angle of attack at station x caused by the traveling gust profile can be expressed as

$$\alpha(t) = w_G(t - (x - x_0)/V)/V \tag{23}$$

whose frequency-domain counterpart is

$$\alpha(i\omega) = (w_G(i\omega)/V)\exp(-i\omega(x - x_0)/V) \tag{24}$$

The resulting generalized force vector caused by a single sinusoidal gust with amplitude $w_G(i\omega)$ and a reference point at x_0 is

$$\big\{p_h^G(i\omega)\big\} = -(q_\infty/V)\{Q_{\rm hG}(ik)\}w_G(i\omega) \tag{25}$$

where

$$\{Q_{\rm hG}(ik)\} = [Q_{\rm hj}(ik)]\{\phi_{\rm jG}(ik)\} \tag{26}$$

where the complex gust mode $\{\phi_{\rm jG}(ik)\}$ and the interim aeromatrix $[Q_{\rm hj}(ik)]$ are

$$\{\phi_{\rm jG}(ik)\} = \begin{Bmatrix} \vdots \\ -n_{z_j} e^{-ik[(x_j - x_0)/L]} \\ \vdots \end{Bmatrix}$$

$$[Q_{\rm hj}(ik)] = [\phi_{\rm kh}]^T[Q_{\rm kj}(ik)]$$

where the index j relates the j-set control points located at x_j, the index k relates to the panel displacements and rotations at the force

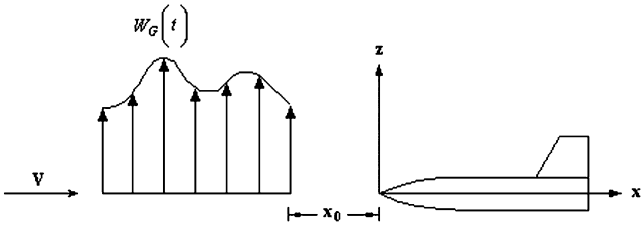

Fig. 1 Traveling excitation caused by the discrete gust profile.

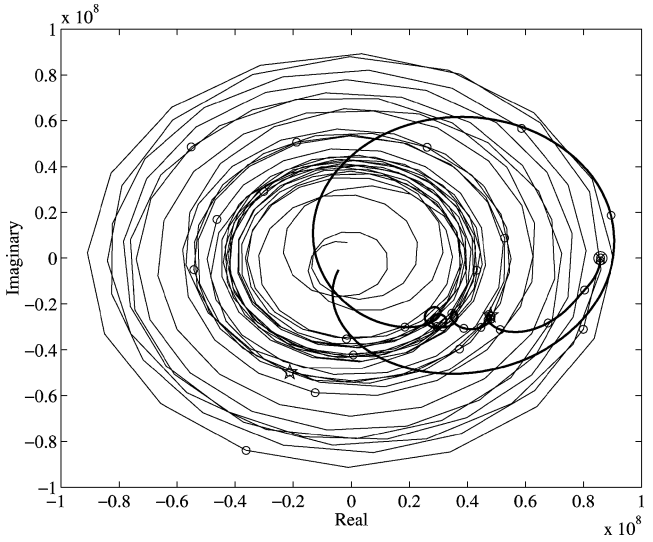

Fig. 2 Variation of sample aerodynamic gust-column term with k, calculated with a) $x_0 = -51.4$ m and b) $x_0 = 6.9$ m (apex point).

points, and n_z is the normal vector component of the aerodynamic box along the gust direction. It can be observed that the complex terms of $\{\phi_{jG}\}$ define the phase shift in gust loads between the reference point and the particular panel control point. When $x - x_0$ is relatively large, the phase changes rapidly with k, which exhibits a spiral shape at high frequencies when the term variation with k is plotted in the Re-Im plane. The variation of a sample Q_{hG} term with k, taken from the numerical example discussed next, is shown in Fig. 2. When the reference point is 51.4 m ahead of the vehicle nose (the thin line), the variation curve exhibits a very spiral behavior. This curve cannot be adequately approximated by a rational function of the form of Eq. (14). The choice of a reference point at the wing leading edge (the thick line) eliminates most of the spiral behavior in this case, especially at low frequencies where the response is most significant. The stars in the plots mark the k value, which corresponds to the wing-bending natural frequency. The circles mark the k values at which data were calculated by the ZAERO code. It can be noticed that the absolute values of corresponding data points are the same along the two lines, which indicates that the choice of reference point would not affect the aerodynamic forces at tabulated k values. Interpolation between tabulated points, however, must consider the spiral nature of the curves.

Discrete Gust Response via Fourier Transforms

With the aerodynamic influence coefficient matrices defined in the frequency domain, a convenient method for solving the response of a structure to discrete gusts is the Fourier transform method adopted by NASTRAN.[2] Fourier transform of $f(t)$ can be expressed as

$$F(i\omega) = \int_{-\infty}^{\infty} f(t)e^{-i\omega t}\,\mathrm{d}t = \Im(f(t)) \tag{27}$$

The inverse of the Fourier transform $F(i\omega)$ is

$$f(t) = \frac{1}{2\pi}\int_{-\infty}^{\infty} F(i\omega)e^{+i\omega t}\,\mathrm{d}\omega = \Im^{-1}(F(i\omega)) \tag{28}$$

where t is the physical time in seconds and ω is the oscillatory frequency in rad/sec.

The response analysis starts with transforming the input gust vector to the frequency domain

$$w_G(i\omega) = \Im(w_G(t)) \tag{29}$$

Equation (11), with s replaced by $i\omega$, is then solved for the state vector

$$\{X_v(i\omega)\} = ([\bar{A}_v(i\omega)] - [I]i\omega)^{-1}[\bar{B}_{vw}(i\omega)]\{w_G(i\omega)\} \tag{30}$$

which can be used for calculating the required plant output values $\{y_R(i\omega)\}$ similarly to $\{y_p(i\omega)\}$ of Eq. (7).

Time-domain response parameters can now be calculated by performing inverse-Fourier transforms

$$\{y_R(t)\} = \Im^{-1}\{y_R(i\omega)\} \tag{31}$$

Subsequent dynamic loads procedures are based on the structural modal displacements, velocities, and accelerations. These are calculated by

$$\{\xi(t)\} = \Im^{-1}\{\xi(i\omega)\}, \qquad \{\dot{\xi}(t)\} = \Im^{-1}(i\omega\{\xi(i\omega)\})$$
$$\{\ddot{\xi}(t)\} = \Im^{-1}(-\omega^2\{\xi(i\omega)\}) \tag{32}$$

with $\{\xi(i\omega)\}$ taken from $\{X_v(i\omega)\}$ of Eq. (29).

Discrete Gust Response via Time-Domain Simulation

The open-loop state-space equations (17), with the $\{u_{ae}\}$ input terms ignored, or the closed-loop equations (22) can be used for direct simulation of the time response to discrete gust excitation, performed by a straightforward numerical simulation. Once constructed, these equations are very efficient and can be used by standard simulation and control-design tool boxes such as MATLAB®. For clarity and simplicity, a single gust velocity profile is assumed in this section. The input vector $\{\tilde{w}_G(t)\}$ is based in this cases on the user-defined gust velocity history $w_G(t)$ at the reference point x_0 and its derivative $\dot{w}_G(t)$. The modal response vectors $\{\xi(t)\}$ and $\{\dot{\xi}(t)\}$ are parts of the open-loop state vector $\{x_{ae}(t)\}$ or the closed-loop one $\{x_v(t)\}$ obtained by the numerical integration. The modal acceleration response $\{\ddot{\xi}(t)\}$ can be derived from the state and input vectors by the second row block of Eq. (22).

The main disadvantage of the time-domain approach, relative to the Fourier-transform one, is that the state-space modeling process requires the unsteady aerodynamic force coefficient matrices to be approximated by rational functions of the Laplace variable [see Eq. (14)]. Any approximation might reduce the accuracy in subsequent analysis, relative to methods that do not require approximations. Nevertheless, the minimum-state approximation processes described in Ref. 7 and applied in Ref. 5 have been shown to be fairly robust and adequately accurate for typical aeroelastic stability and response applications when applied to the modal and control aeromatrices $[Q_{hh}(ik)]$ and $[Q_{hc}(ik)]$. However, rational approximations of the gust-related matrix $[Q_{hG}(ik)]$ might be problematic because of the high-frequency spiral nature of the gust terms when x_0 is located far ahead of some panels of the aeromodel, as discussed earlier. The solution for this problem is obtained by dividing the aerodynamic model into n_{zone} aerodynamic zones (i.e., sets of aerodynamic panels) each having its own reference point x_{0_i}. The gust velocity profile $w_G(t)$ is replaced by several synchronized gusts of time-shifted profiles applied to the different zones,

$$w_{G_i}(t) = w_G(t - (x_{0_i} - x_0)/V) \tag{33}$$

The associated gust mode $\{\phi_{jG}(ik)\}$ is replaced by n_{zone} gust modes

$$\{\phi_{jG_i}(ik)\} = \begin{Bmatrix} \vdots \\ -K_{ji}n_{z_j}e^{-ik[(x_j - x_{0_i})/L]} \\ \vdots \end{Bmatrix} \tag{34}$$

where $K_{ji} = 1$ when the jth panel belongs to the ith zone and $K_{ji} = 0$ when it does not. The x_{0_i} values should be selected such that the $x_j - x_{0_i}$ values for each zone are small enough to prevent gust-mode spirals in the frequency range of interest. With the new gust modes, the single gust column $\{Q_{hG}(ik)\}$ of Eq. (17) becomes a gust matrix $[Q_{hG}(ik)]$ of n_{zone} columns where the ith one is

$$\{Q_{hG_i}(ik)\} = [Q_{hj}(ik)]\{\phi_{jG_i}(ik)\} \tag{35}$$

The rational function approximation with the new tabulated $[Q_{\text{hG}}(ik)]$ matrices yields a different column in the $[A_{\text{hG}n}]$ and $[E_G]$ matrices of Eq. (14) for each aerodynamic zone. The $\{\tilde{w}_G\}$ vector in the equations of motion, (17) or (22), has now $2n_{\text{zone}}$ terms: the $w_{G_i}(t)$ inputs of Eq. (32) and their time derivatives $\dot{w}_{G_i}(t)$.

The replacement of a two-term gust input vector by an input vector with $2n_{\text{zone}}$ terms does not yield significant difficulties in subsequent time simulations. However, it might create difficulties when used in continuous gust response or in control design schemes. To return to a two-term-input situation, the time delays can be represented by approximate delay filters that are augmented to the state-space equations. The nth order approximation of a pure time delay T in the Laplace domain is[9]

$$e^{-Ts} \cong 1/[1 + (Ts/n)]^n \tag{36}$$

which can be realized by state-space equations. When we have, for example, a gust input generated with two aerodynamic zones, the inputs associated with the second zone can be related to those of the first one by the first-order approximation filter, Eq. (35) with $n = 1$,

$$\dot{x}_f = -\frac{1}{T}x_f + \begin{bmatrix} \frac{1}{T} & 0 \end{bmatrix} \begin{Bmatrix} w_{G_1} \\ \dot{w}_{G_1} \end{Bmatrix}$$

$$\begin{Bmatrix} w_{G_2} \\ \dot{w}_{G_2} \end{Bmatrix}^{(1)} = \begin{bmatrix} 1 \\ -\frac{1}{T} \end{bmatrix} x_f + \begin{bmatrix} 0 & 0 \\ \frac{1}{T} & 0 \end{bmatrix} \begin{Bmatrix} w_{G_1} \\ \dot{w}_{G_1} \end{Bmatrix} \tag{37}$$

where $T = (x_{0_2} - x_{0_1})/V$.

An nth order approximation is obtained by connecting n filters of Eq. (36) in series. The result will be an nth order state-space realization of the form

$$\{\dot{x}_f\} = [A_f]\{x_f\} + [B_f]\{\tilde{w}_{G_1}\}$$

$$\begin{Bmatrix} w_{G_2} \\ \dot{w}_{G_2} \end{Bmatrix}^{(n)} = [C_f]x_f + [D_f]\{\tilde{w}_{G_1}\} \tag{38}$$

where $\{\tilde{w}_{G_1}\} = \lfloor w_{G_1} \;\; \dot{w}_{G_1} \rfloor^T$. The augmentation of Eq. (37) to the closed-loop equation (22) yields

$$\begin{Bmatrix} \dot{x}_v \\ \dot{x}_f \end{Bmatrix} = \begin{bmatrix} \bar{A}_v & \bar{B}_{\text{vw}_2} C_f \\ 0 & A_f \end{bmatrix} \begin{Bmatrix} x_v \\ x_f \end{Bmatrix} + \begin{bmatrix} \bar{B}_{\text{vw}_1} + \bar{B}_{\text{vw}_2} D_f \\ B_f \end{bmatrix} \{\tilde{w}_{G_1}\} \tag{39}$$

which has n states more than the original one. A delay approximation with $n = 3$ is typically accurate enough for gust response problems. With more than two aerodynamic zones, several filters of the form of Eq. (37) can be connected to $\{\tilde{w}_{G_1}\}$ in parallel.

Discrete Gust Response by a Hybrid Approach

A hybrid approach that combines the Fourier-transform and the time-domain approaches is presented. The purpose of this approach is to obtain a time-domain state-space model without performing rational approximation to the spiral gust columns. The Fourier transform of the gust profile is first multiplied by the frequency-domain gust column. Inverse-Fourier transforms are then performed to generate the time-domain generalized gust excitation vector. The resulting open-loop state-space matrices are those of Eq. (17) with the gust term $[B_{\text{aw}}]\{\tilde{w}_G\}$ replaced by

$$[B_{\text{aHyb}}]\{w_{\text{Hyb}}(t)\} = \begin{bmatrix} 0 \\ -\frac{q_\infty}{V}[M_{\text{hh}}]^{-1} \\ 0 \end{bmatrix} \Im^{-1}\left(\left\{ Q_{\text{hG}}\left(\frac{i\omega L}{V} \right) \right\} \Im(w_G(t)) \right) \tag{40}$$

where the number of gust input terms is equal to the number of modes taken into account. The resulting hybrid version of the open loop Eq. (17), or that of the closed-loop Eq. (22), are then integrated for the required gust response parameters.

A detailed description of the hybrid approach with numerical verification is given in Ref. 10. The main disadvantages of the hybrid approach are that it has a relatively large input vector, which might be impractical when the model is used in a control design process, and that it involves a relatively large number of Fourier-transform evaluations.

Frequency-Domain Continuous Gust Response

Continuous gust response analysis is commonly performed in the frequency domain.[1,2] The key equations are given here for the sake of completeness. Frequency response functions of the vehicle states can be calculated by Eq. (29) with a single input parameter $w_G = 1$. Any required response parameter can then be obtained by

$$y_R(i\omega) = [C_R]\{X_v(i\omega)\} \tag{41}$$

The PSD function of the response parameter can then be calculated by

$$\Phi_{y_R}(\omega) = |y_R(i\omega)|^2 \Phi_{w_G}(\omega) \tag{42}$$

where $\Phi_{w_G}(\omega)$ is the PSD function of the input gust velocity. The associated rms value of the response can be calculated by

$$\sigma_{y_R} = \sqrt{\frac{1}{\pi}\int_0^\infty \Phi_{w_G}(\omega)\,\mathrm{d}\omega} \tag{43}$$

Continuous Gust Response via State-Space Formulation

A detailed description of continuous gust response analysis using the time-domain state-space ASE formulation is given in Ref. 8. The analysis is based on the addition of a gust filter that yields an ASE system that is excited by a white-noise process input w. The augmentation of the gust-response equation of motion (38) by the gust filter yields

$$\begin{Bmatrix} \dot{x}_v \\ \dot{x}_f \\ \dot{x}_g \end{Bmatrix} = \begin{bmatrix} \bar{A}_v & \bar{B}_{\text{vw}_2} C_f & (\bar{B}_{\text{vw}_1} + \bar{B}_{\text{vw}_2} D_f) C_g \\ 0 & A_f & B_f C_g \\ 0 & 0 & A_g \end{bmatrix} \times \begin{Bmatrix} x_v \\ x_f \\ x_g \end{Bmatrix} + \begin{Bmatrix} 0 \\ 0 \\ B_g \end{Bmatrix} w \tag{44}$$

which can be used for gust response analysis using Lyapunov's equation

$$[A][X] + [X][A] = -\{B_w\}\{B_w\}^T \tag{45}$$

where $[A]$ and $[B_w]$ are the dynamic and input matrices in Eq. (40) and $[X]$ is the covariance matrix of the state vector. The solution of Eq. (44) for $[X]$ yields the covariance matrix of the output vector $\{y_R\}$ of Eq. (40),

$$[Y_R] = [C_R][X][C_R]^T \tag{46}$$

The output covariance matrix can be used for calculating stochastic output parameters such as rms values, number of positive zero crossings, and equal probability ellipses.[1,8] The main advantages of the state-space continuous gust formulation are that it avoids potential difficulties associated with the numerical integration of Eq. (42), its efficiency when applied with a large number of output parameters (all based on the same $[X]$), and its efficiency and convenience when applied for sensitivity analysis in optimization processes.[8]

Numerical Example

The various options for calculating the dynamic response of flight vehicles to atmospheric gusts were integrated it the ZAERO aeroelastic package. They are demonstrated here using the aeroelastic model of a generic transport aircraft (GTA) with a straight wing and a T-tail. The structural stick model for calculating normal modes using MSC/NASTRAN is shown in Fig. 3. The weight of the model is 7203.7 kg. The wing span is 19.0 m, the uniform chord length is 2.3 m, and the length and height of the aircraft are 22.0 m and 6.0 m, respectively. The model contains 117 grid points and 137 structural elements.

The ZAERO unsteady aerodynamic model is shown in Fig. 4. The lifting surfaces are divided into aerodynamic panels with each panel containing several spanwise and chordwise divisions that define the elementary aerodynamic boxes. The model of each wing consists of five aerodynamic panels representing four parts of the wing and the aileron, the model of each side of the horizontal tail contains three panels representing two parts of the tail and the elevator, and the model of the vertical tail contains three panels that represent two parts of the tail and the rudder. The fuselage is represented by body elements. The full model contains 894 aerodynamic boxes. Seventeen aerodynamic force coefficient matrices at reduced frequency values between $k = 0$ and 3.0 were calculated at Mach 0.3.

Discrete and continuous response analyses to symmetric gusts were performed at $V = 200$ kn, sea level. The streamwise gust reference point was $x_0 = 6.9$ m, where the wing's leading edge is located. The frequency range for the frequency-domain options was 0 to 50 Hz. The discrete gust velocity at the reference point was

$$w_G = (\bar{w}_G/2)[1 - \cos(2\pi f t)] \tag{47}$$

with $\bar{w}_G = 100$ ft/s and $f = 11$ Hz. The time window for transient analysis was -0.5 to 1.0 s. The continuous gust analysis was performed with Dryden's PSD of the input gust velocity[5] with rms value of $\sigma_{w_G} = 100$ ft/s and a turbulence scale of $L_G = 2500$ ft.

Nine symmetric modes including two rigid-body modes (heave and pitch) were used in the gust response analysis. Minimum-state rational approximations of the AFC matrices were used for the state-space and the hybrid modeling approaches with nine approximation roots that added nine aerodynamic states.

The control system was based on the application of the two ailerons symmetrically. The state-space plant model was obtained by augmenting the aeroelastic model with third-order models of the two aileron actuators. A single output was that of an accelerometer located at the tip of the right wing. The resulting model was of 33 states, two gust inputs (w_G and $\dot{w}_G$), two identical control inputs, and one sensor output.

The state-space plant model was generated by ZAERO and exported to for control design using MATLAB. Two different control systems were designed, a simple single-input single-output system and a more complicated one based on H_∞ concepts. The simple system was designed to reduce the measured wing-tip acceleration in response to the discrete-gust excitation as much as possible without exceeding the maximal control-surface deflection of 20 deg. The resulting system is based on a low-pass filter T_{lpf} supplemented by a notch filter T_{nf} to prevent unfavorable interaction with the lowly-damped fuselage bending mode at about 32 Hz,

$$T(s) = T_{\text{lpf}} T_{\text{nf}} = \frac{8 \cdot 10^5}{s + 100} \times \frac{s^2 + 10s + 4 \cdot 10^4}{s^2 + 200s + 4 \cdot 10^4} \tag{48}$$

The H_∞ controller was designed using the MATLAB μ-Analysis and Synthesis Toolbox. The goal was to minimize the rms value of the wing-tip acceleration in response to the Dryden gust spectrum just described with control-surface rms deflection of 5.7 deg. The H_∞ design resulted in a control system with 21 states. The maximal closed-loop response of the control surface to the discrete gust excitation of Eq. (46) was about 25 deg.

The two control systems used in ZAERO analyses were the wing-tip acceleration and the wing-root shear force, and bending moment and torsion moment were monitored in open- and closed-loop discrete and continuous gust response analyses.

The results of the discrete gust response analysis are shown in Figs. 5–7. It can be observed that all of the three methods, frequency-domain, state-space, and hybrid, gave very close results. A comparison of the maximal absolute values of the wing-tip accelerations obtained by the three methods is given in Table 1. It can be observed that the peak values obtained by the state-space and hybrid methods compare well with the frequency-domain results, and that significant reductions were obtained by the application of the control laws.

Power-spectral-density variations of the wing-tip acceleration obtained in frequency-domain continuous gust response analyses are shown in Fig. 8. RMS values of the wing tip acceleration obtained by the application of frequency-domain and state-space methods are shown in Table 1. Here again, the control systems are effective, and the state-space results compare well with the frequency-domain ones.

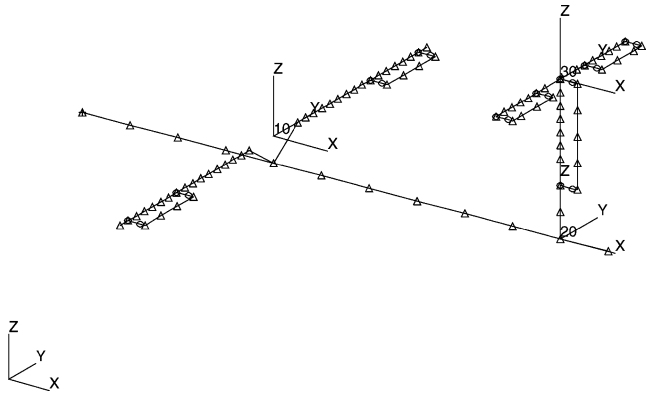

Fig. 3 GTA structural model.

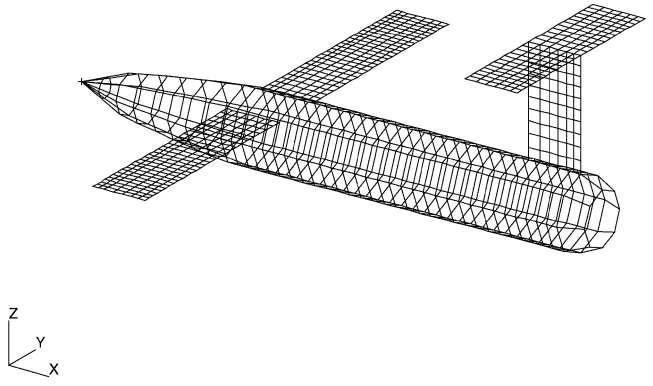

Fig. 4 GTA aerodynamic model.

Table 1 Wing-tip acceleration caused by discrete and continuous gusts

	Maximal acceleration caused by discrete gust, m/s^2					RMS acceleration caused by continuous gust, m/s^2		
Case	Freq. domain	State space	Error, %	Hybrid	Error, %	Freq. domain	State space	Error, %
Open loop	479.9	484.8	1.0	484.6	1.0	58.24	59.93	2.9
Simple control	360.4	367.0	1.8	369.0	2.4	49.36	50.18	1.7
H_∞ controller	177.8	184.3	3.7	183.0	2.9	31.40	32.55	3.7

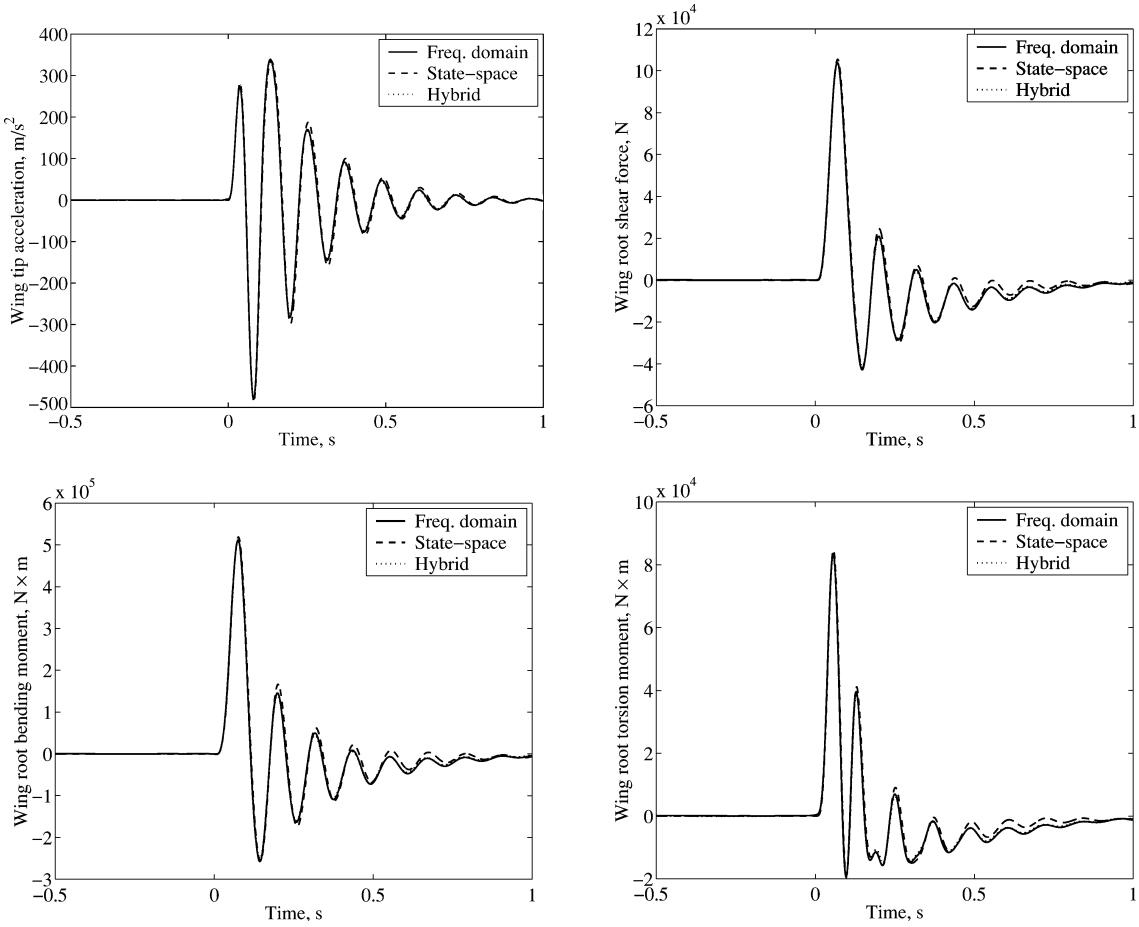

Fig. 5 Open-loop discrete gust response.

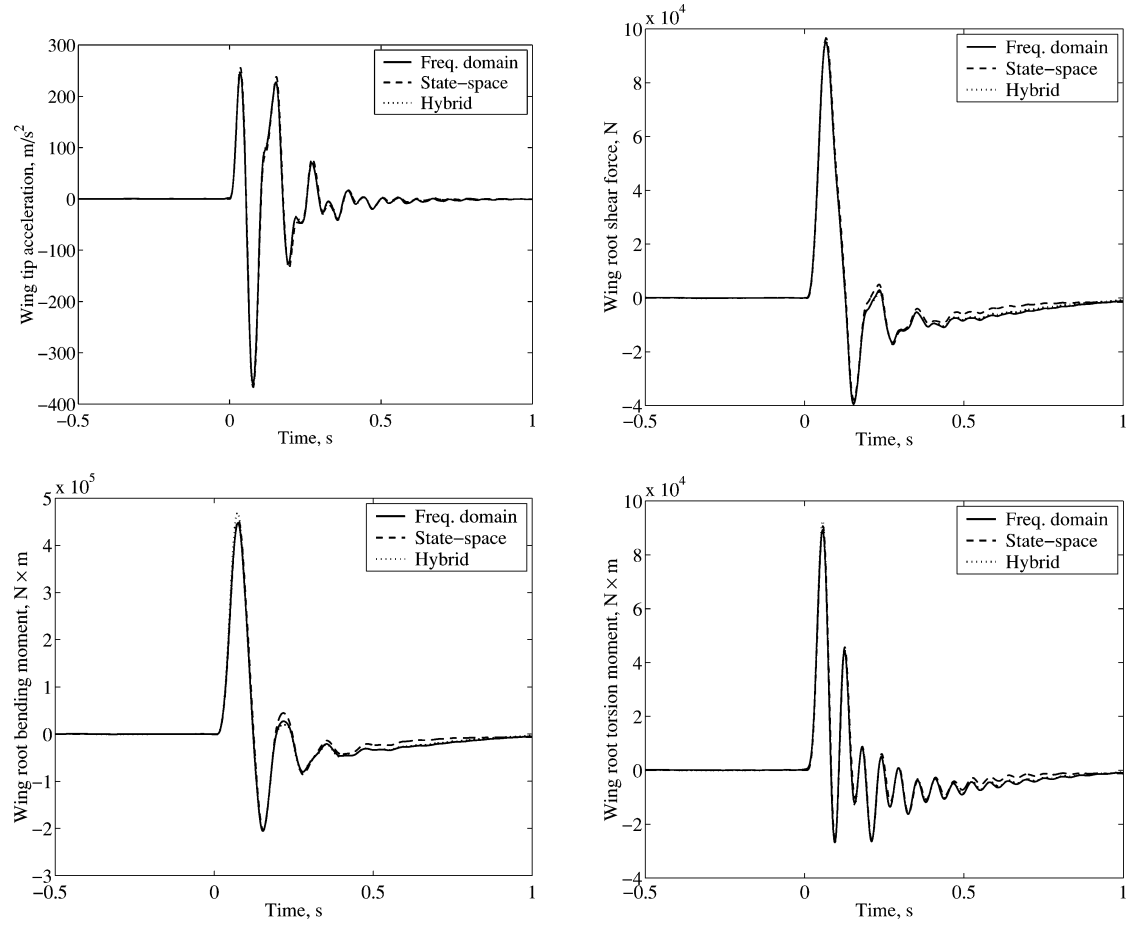

Fig. 6 Closed-loop discrete gust response, third-order simple controller.

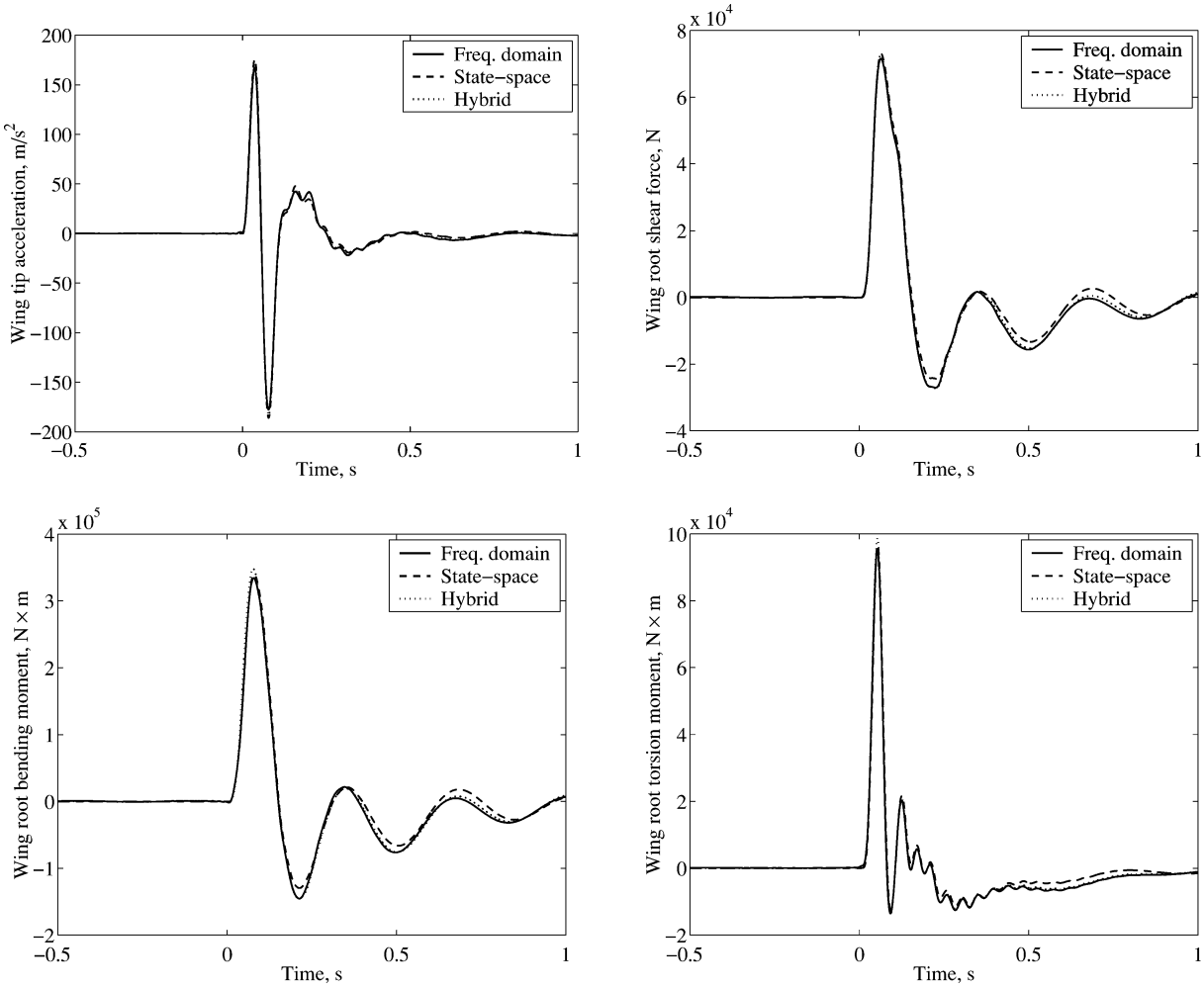

Fig. 7 Closed-loop discrete gust response, H_∞ controller.

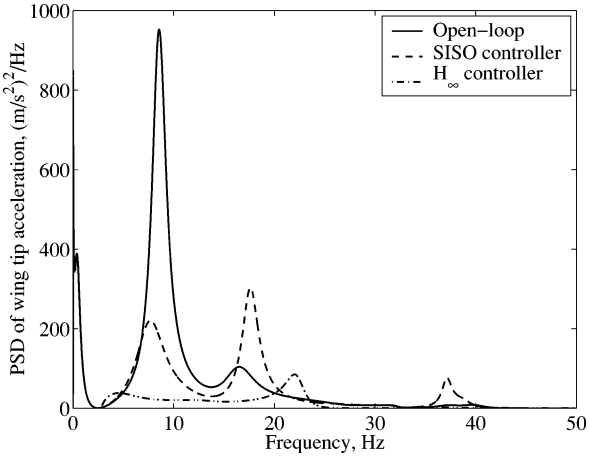

Fig. 8 PSD of wing-tip acceleration response to continuous gust.

Conclusions

Frequency-domain and time-domain approaches were formulated and applied to dynamic discrete and continuous gust response analyses of aeroservoelastic systems to atmospheric gust excitations. A linear control system of the most general form can be included in the analysis. The frequency-domain approach is based on the interpolation of generalized aerodynamic-force-coefficient matrices calculated by common unsteady aerodynamic routines at tabular reduced-frequency values. The interpolation scheme considers the special spiral nature of the gust-related coefficients. The time-domain approach is based on constant-coefficient state-space formulation, which requires the approximation of the aerodynamic coefficients by rational functions of the Laplace variable. The approximation might degrade the resulting accuracy, but it typically yields considerably more efficient models and better suitability to the application of modern control techniques. Rational approximation problems associated with the spiral nature of the gust columns can be alleviated by dividing the aerodynamic model into several aerodynamic zones. A hybrid approach is also presented for discrete gust response analysis. The hybrid approach can be more accurate in some cases because it does not require the rational approximation of the gust columns. However, it might be less efficient in subsequent simulations and less suitable for control applications because of the relatively large number of input parameters. The various methods were utilized in the ZAERO software and applied to a generic transport aircraft model. The results exhibited good agreement between the various methods. A practical scenario of model generation, control system design, and gust response analysis was demonstrated.

Acknowledgments

The work presented in this paper was partially supported by European Aerospace Defense Systems-Construcciones Aeronauticas, S.A. (EADS-CASA). The excellent advise, technical support, and numerical data provided by Hector Climent, Carlos Maderuelo, and Luis Anguita of EADS-CASA are gratefully acknowledged.

References

[1]Hoblit, F. M., *Gust Loads on Aircraft: Concepts and Applications*, AIAA Education Series, AIAA, Washington, DC, 1988.

[2]Rodden, W. P., and Johnson, E. H., "MSC/NASTRAN Aeroelastic Analysis User's Guide," The MacNeal-Schwendler Corp., Los Angeles, 1994.

[3]Rodden, W. P., Taylor, P. F., and McIntosh, S. C., Jr., "Further Reinment of the Nonplanar Aspects of the Subsonic Doublet-Lattice Lifting Surface Method," *Journal of Aircraft*, Vol. 35, No. 5, 1998, pp. 720–727.

[4]Liu, D. D., Chen, P. C., Yao, Z. X., and Sarhaddi, D., "Recent Advances in Lifting Surface Methods," *The Royal Aeronautical Journal*, Vol. 100, No. 998, Oct. 1996, pp. 327–339.

[5]*ZAERO Version 6.2 Theoretical Manual*, ZONA Technology, Inc., ZONA 02-12.4, Scottsdale, AZ, Oct. 2002.

[6]Roger, K. L., "Airplane Math Modeling for Active Control Design," *Proceedings of the 44th AGARD Structures and Materials Panel*, AGARD-CP-228, April 1977, pp. 4.1–4.11.

[7]Karpel, M., "Time Domain Aeroservoelastic Modeling Using Weighted Unsteady Aerodynamic Forces," *Journal of Guidance, Control, and Dynamics*, Vol. 13, No. 1, 1990, pp. 30–37.

[8]Zole, A., and Karpel, M., "Continuous Gust Response and Sensitivity Derivatives Using State-Space Models," *Journal of Aircraft*, Vol. 31, No. 5, 1994, pp. 1212–1214.

[9]Kuo, B. C., *Automatic Control Systems*, Prentice–Hall, Englewood–Cliffs, NJ, 1982, pp. 454–456.

[10]Chen, P. C., "Nonhomogeneous State-Space Approach for Discrete Gust Analysis of Open-Loop/Closed-loop Aeroelastic Systems," AIAA Paper 2002-1715, April 2002.

[11]Karpel, M., and Presente, E., "Structural Dynamic Loads in Response to Impulsive Excitation," *Journal of Aircraft*, Vol. 32, No. 4, 1995, pp. 853–861.